Supplementary Material

Echocardiography protocol:

Conventional measures of left ventricular function and dimensions:

Left ventricular systolic function was measured using ejection fraction, and calculated according to the modified Simpson's rule in apical 4 chamber view[1]. Method of disks (modified Simpson's rule) was used to estimate left ventricular end-diastolic volume and end-systolic volume from the 4-chamber endocardial area tracing. Early on Late (E/A) peak velocity ratio of the mitral valve inflow was calculated using the Pulsed-Wave Doppler sampled below the valve in the apical 4 chamber view.

Conventional measures of right ventricular function and dimensions:

Fractional area change of the right ventricle was calculated from the endocardial area tracing of the right ventricle at end-diastole and end-systole in apical 4 chamber view[2]. Tricuspid annular plane systolic excursion was measured from the lateral border of the tricuspid valve, from end-diastole to end-systole in apical 4 chamber view [3]. A tricuspid annular plane systolic excursion below 7 mm was established as the cut-off value for abnormal right ventricular function [4]. Tricuspid annular plane systolic excursion had a good inter-reader reproducibility by Bland–Altman plot and Pearson's correlation in a previous report by our group, using the same methodology[5]. Early on Late (E/A) peak velocity ratio of the tricuspid valve inflow was calculated using the Pulsed-Wave Doppler sampled below the valve in the apical 4 chamber view. Measurements of the right ventricular dimensions (tricuspid valve, basal diameter, mid-cavity diameter and longitudinal dimension) were done at end diastole, according to the American Society of Echocardiography [6].

Tissue Doppler Imaging:

Highest systolic myocardial (s') and early diastolic (e') velocities, isovolumetric contraction time, isovolumetric relaxation time and right or left ventricular ejection time were derived from the tissue Doppler imaging obtained from the lateral wall of the left ventricle and the free wall of the right ventricles in the apical 4 chamber view [7]. The myocardial performance index of the right and left ventricles, an index of combined systolic and diastolic performance, was derived using the tissue Doppler imaging tracing and according to: (isovolumetric contraction time + isovolumetric relaxation time)/Ejection time of the corresponding ventricle [8].

Stroke distance and estimated outputs:

The velocity time integral of the pulsed wave Doppler envelope in the right ventricular outflow tract, sampled at the level of the pulmonary valve attachments, was measured in the parasternal short axis view to estimate stroke distance. Left ventricular outflow tract velocity time integral of the pulsed wave Doppler, sampled at the level of the aortic valve attachments, was measured in the apical 3-chamber view. Right ventricular stroke distance by velocity time integral had adequate inter-reader reproducibility by Bland–Altman plot and Pearson's correlation in a previous study by our group using the same methodology [5].

Pulmonary artery pressure estimation

Systolic pulmonary arterial pressure was estimated using the Bernoulli equation applied to either: a) tricuspid regurgitant jet (when a full Doppler envelope was available) and adding an estimated right atrial pressure of 5 mmHg, or b) by a restrictive ventricular septal defect or a patent ductus arteriosus velocity gradient [3]. Since these measurements were obtained during early neonatal life, a ratio of the estimated peak systolic pulmonary arterial pressure to systolic systemic blood pressure at the time of the echocardiography was also calculated. Supra-systemic pulmonary pressures were defined as systolic pulmonary arterial pressure / systolic systemic blood pressure ratio > 110%. Pulmonary artery acceleration time to right ventricular ejection time ratio was measured from the pulsed wave Doppler of the right ventricular outflow tract in parasternal short axis view (at the tip of the valve). A pulmonary artery acceleration time to right ventricular ejection time ratio less than 0.30 has been described as a marker of pulmonary vascular disease [3, 9]. Left ventricular eccentricity index at the peak of systole, a quantification of septal distortion and right-left ventricular crosstalk, was calculated in parasternal short axis view at papillary muscle level [3]. Eccentricity index is the ratio between the largest measurement of the left ventricle parallel to the interventricular septum to the largest measurement perpendicular to the interventricular septum (with a perfect circle providing a ratio of 1). [2, 9, 10] Values ≥ 1.3 have been associated with right ventricular systolic dysfunction in newborns[11]. Main pulmonary artery was measured as the largest diameter in the suprasternal notch view or parasternal short-axis view. As a measure of right ventricular dilation, the right to left ventricular ratio was calculated (ratio between the distance from the interventricular septum to the right ventricular free wall to the distance of interventricular septum to the left ventricular free wall at end of systole in parasternal short axis at papillary level) [12].

Deformation analysis of ventricular function

Stored Digital Imaging and Communications in Medicine images of the apical 4 chamber view were transferred to the Velocity Vector Imaging (VVI 3.01.45 by Siemens Medical Solutions, United States, Mountain View, California) platform for deformation analysis by speckle-tracking echocardiography[13]. Speckle-tracking echocardiography tracks the endocardial border to estimate global and segmental cardiac performance by % deformation (strain) or rate of deformation (1/second)[14]. Right and left ventricular endocardial tracing were done manually and repeated to ensure appropriate tracking[15]. The interventricular septum was included in each ventricle. Images were stored between 30 and 60 frames per second [16]. R waves of the QRS were indicated on the platform from the electrocardiogram data inputted into the Digital Imaging and Communications in Medicine images and two to three consecutive cardiac cycles were used for analysis. Peak longitudinal strain and peak longitudinal strain rate were provided by the platform, while peak early diastolic strain rate was extracted from the average strain rate curve [14, 17, 18]. When peak early and peak late diastolic strain rate curves were fused, as it is often the case in the neonatal period, peak diastolic strain rate was collected as the early diastolic strain rate. Right ventricular peak longitudinal strain of -14% and left ventricular peak longitudinal strain of -16% were considered as cut-off for abnormal, based on a previous neonatal study [19], which established this value as 1 standard deviation below the mean from newborn control data.

Supplementary Figures:

Figure S1:

A) Association between conventional and speckle-tracking echocardiography markers of systolic function

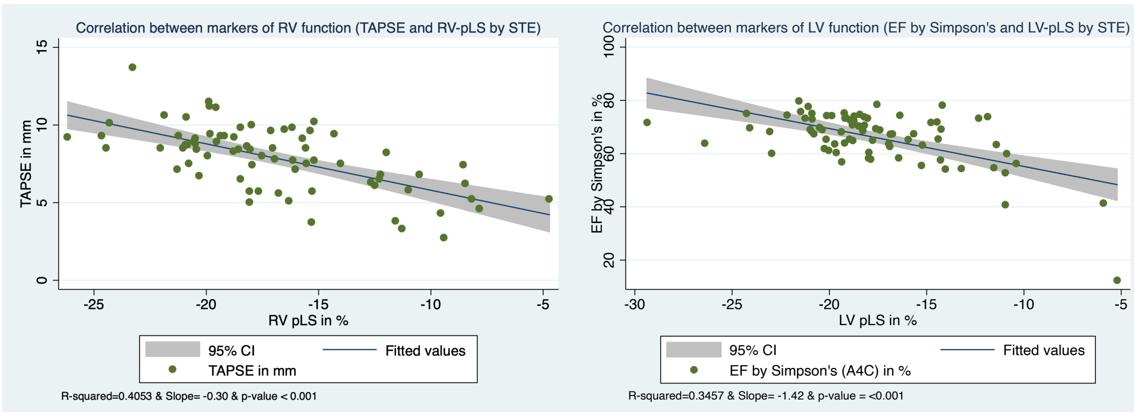

B) Stroke distance by velocity time integral correlates with underlying ventricular deformation

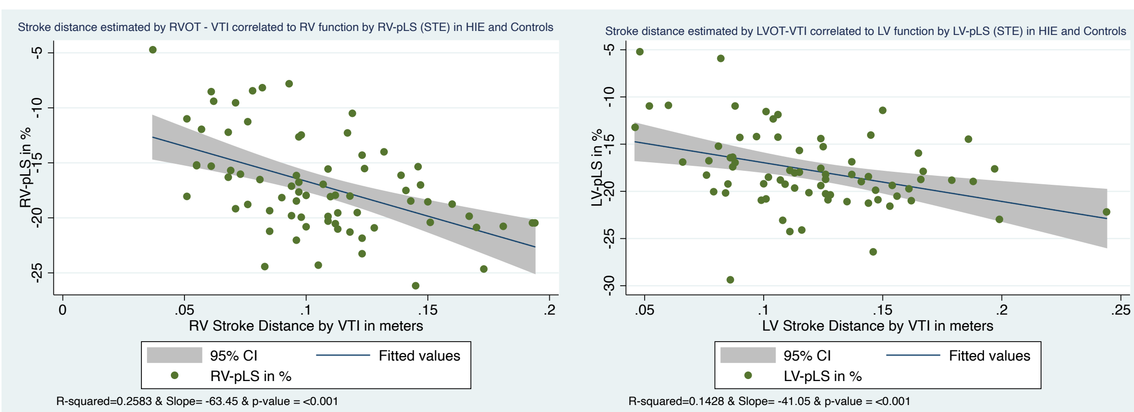

Legend: (A) Tricuspid annular plane systolic excursion (TAPSE), a marker of right ventricular (RV) systolic function, was associated with right ventricular peak longitudinal strain (pLS). Similarly, the ejection fraction (EF) by Simpson's disc method in the apical 4-chamber view (A4C), a conventional echocardiography marker of left ventricular (LV) systolic function, was associated with the left ventricular peak longitudinal strain by speckle-tracking echocardiography (STE). (B) Right and left ventricular stroke distance by velocity time integral (VTI) of the corresponding outflow tract (OT) was associated with the underlying systolic function measured by peak longitudinal strain by speckle-tracking echocardiography. Values for the hypoxic ischemic encephalopathy and control newborns were included in this analysis.

References for Supplementary Material:

1. Kosaraju A, Goyal A, Grigorova Y and Makaryus AN. Left ventricular ejection fraction. 2017.
2. Jone PN and Ivy DD. Echocardiography in pediatric pulmonary hypertension. Front Pediatr 2014; 2: 124.
3. Altit G, Dancea A, Renaud C, Perreault T, Lands LC and Sant'Anna G. Pathophysiology, screening and diagnosis of pulmonary hypertension in infants with bronchopulmonary dysplasia-A review of the literature. Paediatric respiratory reviews 2016.
4. Koestenberger M, Ravekes W, Everett AD et al. Right ventricular function in infants, children and adolescents: reference values of the tricuspid annular plane systolic excursion (TAPSE) in 640 healthy patients and calculation of z score values. J Am Soc Echocardiogr 2009; 22: 715-719.
5. Altit G, Bhombal S, Chock VY and Tacy TA. Immediate Postnatal Ventricular Performance Is Associated with Mortality in Hypoplastic Left Heart Syndrome. Pediatric cardiology 2019; 40: 168-176.
6. Lopez L, Colan SD, Frommelt PC et al. Recommendations for quantification methods during the performance of a pediatric echocardiogram: a report from the Pediatric Measurements Writing Group of the American Society of Echocardiography Pediatric and Congenital Heart Disease Council. Journal of the American Society of Echocardiography 2010; 23: 465-495.
7. Negrine RJ, Chikermane A, Wright JG and Ewer AK. Assessment of myocardial function in neonates using tissue Doppler imaging. Arch Dis Child Fetal Neonatal Ed 2012; 97: F304-306.

8. Chuwa T and Rodeheffer RJ. New index of combined systolic and diastolic myocardial performance: a simple and reproducible measure of cardiac function--a study in normals and dilated cardiomyopathy. J cardiol 1995; 26: 7-366.
9. Nagiub M, Lee S and Guglani L. Echocardiographic assessment of pulmonary hypertension in infants with bronchopulmonary dysplasia: systematic review of literature and a proposed algorithm for assessment. Echocardiography (Mount Kisco, NY) 2015; 32: 819-833.
10. Jone PN and Ivy DD. Comprehensive Noninvasive Evaluation of Right Ventricle-Pulmonary Circulation Axis in Pediatric Patients with Pulmonary Hypertension. Current treatment options in cardiovascular medicine 2019; 21: 6.
11. Jain A, Mohamed A, El-Khuffash A et al. A comprehensive echocardiographic protocol for assessing neonatal right ventricular dimensions and function in the transitional period: normative data and z scores. Journal of the American Society of Echocardiography : official publication of the American Society of Echocardiography 2014; 27: 1293-1304.
12. Koestenberger M, Friedberg MK, Nestaas E, Michel-Behnke I and Hansmann G. Transthoracic echocardiography in the evaluation of pediatric pulmonary hypertension and ventricular dysfunction. Pulmonary circulation 2016; 6: 15-29.
13. Arunamata A, Selamet Tierney ES, Tacy TA and Punn R. Echocardiographic measures associated with early postsurgical myocardial dysfunction in pediatric patients with mitral valve regurgitation. J Am Soc Echocardiogr 2015; 28: 284-293.
14. Lorch SM, Ludomirsky A and Singh GK. Maturational and growth-related changes in left ventricular longitudinal strain and strain rate measured by two-dimensional speckle

tracking echocardiography in healthy pediatric population. J Am Soc Echocardiogr 2008; 21: 1207-1215.

15. Fine NM, Shah AA, Han IY et al. Left and right ventricular strain and strain rate measurement in normal adults using velocity vector imaging: an assessment of reference values and intersystem agreement. Int J Cardiovasc Imaging 2013; 29: 571-580.
16. Bansal M and Kasliwal RR. How do I do it? Speckle-tracking echocardiography. Indian Heart J 2013; 65: 117-123.
17. Carasso S, Biaggi P, Rakowski H et al. Velocity Vector Imaging: standard tissue-tracking results acquired in normals--the VVI-STRAIN study. J Am Soc Echocardiogr 2012; 25: 543-552.
18. Punn R, Axelrod DM, Sherman-Levine S, Roth SJ and Tacy TA. Predictors of mortality in pediatric patients on venoarterial extracorporeal membrane oxygenation. Pediatric critical care medicine: a journal of the Society of Critical Care Medicine and the World Federation of Pediatric Intensive and Critical Care Societies 2014; 15: 870.
19. Patel N, Massolo AC, Paria A et al. Early Postnatal Ventricular Dysfunction Is Associated with Disease Severity in Patients with Congenital Diaphragmatic Hernia. J Pediatr 2018; 203: 400-407.e401.